International Journal of Thermal Sciences 118 (2017) 355–366

Contents lists available at ScienceDirect

International Journal of Thermal Sciences

journal homepage: www.elsevier.com/locate/ijts

Experimental and numerical study of turbulent flow and enhanced heat transfer by cross-drilled holes in a pin-finned brake disc

Hongbin Yan [a], Shangsheng Feng [b, c], Tianjian Lu [b, c, *], Gongnan Xie [a, **]

[a] School of Marine Science and Technology, Northwestern Polytechnical University, Xi'an 710072, PR China
[b] MOE Key Laboratory for Multifunctional Materials and Structures, Xi'an Jiaotong University, Xi'an 710049, PR China
[c] State Key Laboratory for Strength and Vibration of Mechanical Structures, Xi'an Jiaotong University, Xi'an 710049, PR China

ARTICLE INFO

Article history:
Received 18 October 2016
Received in revised form
23 April 2017
Accepted 24 April 2017
Available online 12 May 2017

Keywords:
Ventilated brake disc
Pin-fin
Radial vane
Cross-drilled hole
Heat transfer enhancement

ABSTRACT

This numerical study presents a systematic comparison of the fluid flow and heat transfer characteristics between standard and cross-drilled ventilated brake discs incorporating pin-fins. To validate the numerical model, heat transfer measurement is performed for a commercially available standard brake disc. Within the representative operating range of 200–1000 rpm, results show that the introduction of cross-drilled holes on the rubbing discs enhances the overall cooling capacity of the pin-finned brake disc by 15–17%. As a result of axial pressure gradient, the low-momentum boundary-layer fluid near the rubbing surfaces is driven into the ventilated channel through the cross-drilled holes. Consequently, within radial spans of the cross-drilled holes, local heat transfer on the rubbing surfaces is evidently improved. In addition, the through-hole flow provides substantial heat removal from additional surface of the holes. However, the flow ejected from the cross-drilled holes blocks and interacts with the mainstream entered from the inlet of the ventilated channel, which ultimately reduces the effective flow area and increases resistance to the mainstream. Thus pumping capacity through the inlet of the ventilated channel decreases; and correspondingly, local heat transfer on other surfaces of the rubbing discs is slightly deteriorated. These mutually conflicting mechanisms are responsible for the superior overall cooling performance of the cross-drilled pin-finned brake disc.

1. Introduction

Disc brakes as schematically illustrated in Fig. 1(a) are crucial security equipment in modern passenger vehicles and medium-sized trucks for deceleration. When a driver actuates the brake pedal, sliding friction forms between the brake disc and a pair of brake pads which independently rotate and remain stationary relative to the suspension system. Consequently, a large amount of kinetic and potential energy of the vehicle is transformed into thermal energy during high-load braking, which can lead to overheating of the brake disc. Many studies available in the open literature have shown that such overheating can result in deterioration of friction coefficient [1–3], severe wear of the rubbing surface [4], cracking of the rubbing disc induced by thermal stress [5–7] and thermal judder of the brake system as a result of non-uniform thermal deformation of the brake disc [8]. Consequently, effective and uniform cooling of the brake disc is crucial for disc brake systems.

To improve cooling performance, various ventilated brake discs have been devised and used in modern vehicles. These brake discs generally have a similar structure as those shown in Fig. 1(b). Aerodynamic and heat dissipation elements are sandwiched between two thick rubbing discs. Such brake discs work like centrifugal fans during rotation, sucking cooling air around the brake disc into the ventilated channel. Therefore, better cooling performance can generally be achieved due to the additional forced convection inside the ventilated channel and the enlarged heat transfer area relative to the limited convection near the rubbing surfaces of a solid brake disc [9]. Among the ventilated brake discs with radial vanes, curved vanes and pin-fins, the application of curved vane brake discs are limited since this type of brake disc is unidirectional. In contrast, radial vane and pin-finned brake discs are bidirectional; and the same brake disc can be mounted to any tire of a vehicle.

* Corresponding author. State Key Laboratory for Strength and Vibration of Mechanical Structures, Xi'an Jiaotong University, Xi'an 710049, PR China.
** Corresponding author. School of Marine Science and Technology, Northwestern Polytechnical University, Xi'an 710072, PR China.
E-mail addresses: tjlu@mail.xjtu.edu.cn (T. Lu), xgn@nwpu.edu.cn (G. Xie).

http://dx.doi.org/10.1016/j.ijthermalsci.2017.04.024
1290-0729/

Nomenclature

A	heat transfer area (m^2)
d_h	diameter of the circular cross-drilled holes (m)
d_p	diameter of the circular pin-fins (m)
h	local heat transfer coefficient (W/(m^2K))
h_e	local effective heat transfer coefficient defined in Eq. (4) (W/(m^2K))
$h_{overall}$	overall heat transfer coefficient defined in Eq. (3) (W/(m^2K))
H_{h1}, H_{h2}	axial dimensions of the hub of the brake disc (m)
H_p	height of the pin-fins (m)
k	thermal conductivity of air (W/(mK))
L_p	length of the pin-fins (m)
N	rotational speed of the brake disc (rpm)
Nu	local Nusselt number
Nu_e	local effective Nusselt number defined in Eq. (5)
$Nu_{overall}$	overall Nusselt number defined in Eq. (2)
p	pressure (Pa)
q''	heat flux imposed by each heating pad (W/m^2)
r	radial coordinate (m)
r_{p1}, r_{p2}	round radii of the pin-fins (m)
Re	rotational Reynolds number defined in Eq. (1)
R_{h1}–R_{h4}	radial locations of the cross-drilled holes (m)
R_{hb1}, R_{hb2}	radial dimensions of the hub of the brake disc (m)
R_i, R_o	inner and outer radii of the inboard disc (m)
R_{p1}–R_{p4}	radial locations of the pin-fins (m)
t_r	thickness of the rubbing disc (m)
T	local wall temperature (°C)
T_a	reference air temperature (°C)
T_{rs}	local temperature on the inboard rubbing surface (°C)
$T_{rs,\ m}$	area-averaged rubbing surface temperature (°C)
V	relative velocity magnitude (m/s)
W_p	width of the pin-fins (m)
z	axial coordinate (m)

Greek symbols

ε	emissivity of the matt black paint
η	contribution of separate mechanism to overall heat transfer enhancement
θ	azimuth coordinate (rad)
θ_0	periodic angle of the brake disc (rad)
μ	dynamic viscosity of air (Pa·s)
ρ	density of air (kg/m^3)
σ	Stefan-Boltzmann constant (W/(m^2K^4))
ω	angular velocity magnitude (rad/s)

Although the radial vane brake disc generally has better overall cooling performance than the pin-finned brake disc, the latter such as the one as shown in Fig. 1(b) exhibits better thermal uniformity inside the brake disc due to more uniform distribution of the core elements along both the radial and circumferential directions, which helps to prevent thermal cracking [10,11]. Therefore, both types of brake discs are widely used in modern vehicles [12]. The present study focuses on the pin-finned brake discs.

Commercially available bidirectional ventilated brake discs may be classified into standard and cross-drilled brake discs as shown in Fig. 1(b) [12]. Since 1960s [13], numerous analytical, numerical and experimental studies have been conducted to characterize the thermo-fluidic characteristics of the standard brake disc. In contrast, investigation into the cross-drilled brake disc is limited.

For the standard pin-finned brake disc, Barigozzi et al. [14,15] measured mean velocity and turbulence intensity distributions on several cylindrical cross-sections at the exit of the ventilated channel. The brake disc considered by these authors has diamond and teardrop shaped pin-fins. Jet-like exit flows were reported; and the non-dimensional velocity and temperature distributions were independent of the rotational speed of the brake disc. Wallis et al. [16] investigated numerically the flow characteristics inside a ventilated brake disc with diamond and teardrop shaped pin-fins. It was reported that a low-momentum separated region exists downstream each pin-fin. Manohar Reddy et al. [10] compared numerically the flow and heat transfer characteristics of two brake discs separately with diamond and circular pin-fins. It was found that the former exhibited better cooling performance although the

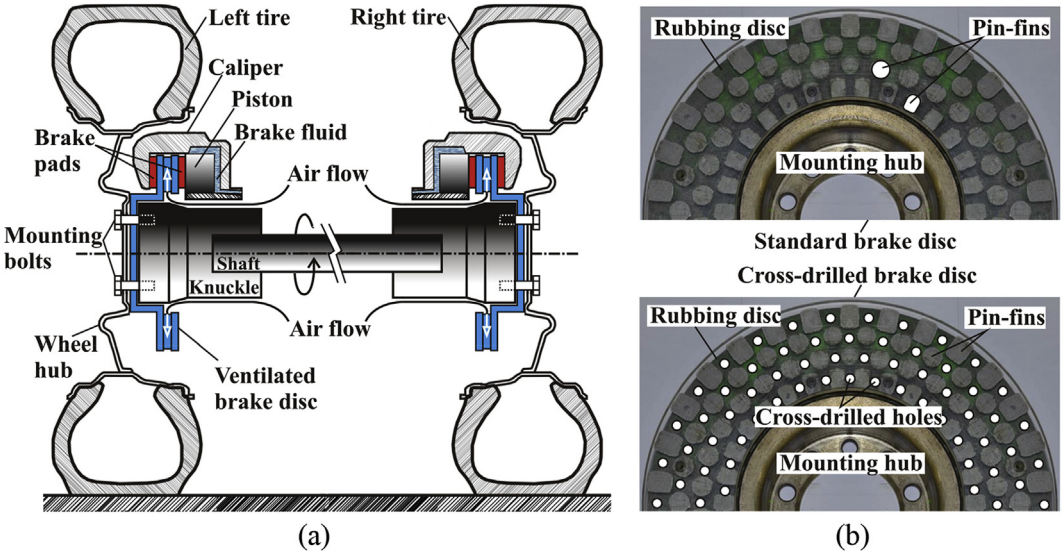

Fig. 1. Illustration of a ventilated disc brake system: (a) the components and working principle; (b) standard and cross-drilled ventilated brake discs with pin-fin elements.

flow patterns of the two brake discs were similar. Palmer et al. [11,17] conducted parametric studies of diamond pin-finned brake discs by using numerical simulations. It was found that cooling performance improved when using thinner pin-fins along the circumferential direction at the inlet of the ventilated channel.

For the cross-drilled brake disc, Wallis [18] compared cooling performance between a standard brake disc and a cross-drilled brake disc by dynamometer testing. It was reported that cross-drilling improved the cooling performance. However, no information regarding the core elements was provided. Antanaitis et al. [19] conducted on-vehicle testing of ventilated brake discs. It was also found that the cross-drilled brake disc had better cooling performance. Unfortunately, the authors deliberately concealed the core elements. Barigozzi et al. [20] measured the flow field near the rubbing surface and at the ventilated channel outlet of a radial vane brake disc made from ceramic composite material. Air was found to enter the ventilated channel through the cross-drilled holes. However, the effects of the through-hole flow on the local flow and heat transfer characteristics were not provided; comparison with the corresponding standard brake disc and the geometric details of the test sample were also missing. In view of the above vague studies, the present authors [21] recently investigated the effects of the cross-drilled holes on the fluid flow and heat transfer characteristics of a widely used radial vane brake disc with geometric details provided. Modification of the internal and external flows as well as local heat transfer on various surfaces of the brake disc by cross-drilled holes was clarified.

In view of the above, it has been well established that different core elements configured in the ventilated channel always lead to distinct flows around the standard brake disc. Once cross-drilled holes are introduced, the through-hole flow will interact with these different external and internal flows in different manners, which ultimately results in different cooling performance. Focusing on this point, this study presents a thorough thermo-fluidic comparison between standard and cross-drilled pin-finned brake discs as shown in Fig. 1(b), which, to the best knowledge of the present authors, has not yet been clearly investigated in the open literature. Heat transfer experiments were conducted on a commercially available pin-finned brake disc to validate the numerical model. Three-dimensional numerical simulations in a rotating environment were conducted for both the standard and cross-drilled brake discs for comparison. Particular focus is placed upon: (a) the qualitative and quantitative effects of the cross-drilled holes on detailed fluid flow and heat transfer behaviors of the pin-finned brake disc; (b) the relative merits among the pin-finned and radial vane brake discs with/without cross-drilled holes and the underlying mechanisms.

It should be noted that the present experiments and numerical simulations were conducted under steady-state conditions. Although a large proportion of braking in the real world is transient, the heat transfer associated with brake discs may approach steady-state during long-time downhill braking or repeated braking. For engineering applications, disc brake systems have to be reliable under all these circumstances. Therefore, the present steady-state analysis is helpful for the design of brake discs.

2. Standard and cross-drilled brake discs investigated

Geometric dimensions of the pin-finned brake discs considered in the present numerical comparison were designed according to a commercial brake disc as shown in Fig. 1(b). However, to ensure a systematic comparison between the standard and cross-drilled brake discs incorporating both the radial vanes and pin-fins, the dimensions are modified and are somewhat different from those of the commercial one. As shown in Fig. 2, the standard brake disc contains 120 pin-fins configured in four rows in a staggered pattern. The two central rows have an identical circular cross-section, while the innermost and outermost rows have blunt ends. The two rubbing discs have an identical thickness (t_r). In particular for the cross-drilled brake disc, four rows of circular holes are drilled through both the rubbing discs. Each hole is located circumferentially at the center of two adjacent pin-fins. The centers of the holes are located radially at $r = 88.3$ mm, 113.4 mm, 127.4 mm and 140.7 mm, respectively. Other dimensions of the cross-drilled brake disc are identical to those of the standard one. Detailed geometric parameters are depicted in Fig. 2 and summarized in Table 1. For the numerical comparison, both brake discs were assumed to be made of grey cast iron. Thermal conductivity of this material is ~42 W/(mK) [22].

3. Experimental details

To ensure a reliable comparison between the standard and cross-drilled brake discs, the numerical model has to be carefully validated. Consequently, heat transfer measurement was conducted on a standard brake disc. It should be mentioned that information about the test sample, test rig and experimental method has been presented in a previous study [23]. For the sake of completeness of this paper, only necessary details are presented below.

3.1. Test sample and test rig

For convenience, a commercial standard brake disc as shown in Fig. 1(b) was selected and tested. This brake disc is made of cast iron with the thermal conductivity of ~42 W/(mK) [22]. Relevant geometric parameters of this specimen are given in Table 2.

The purposely built rotating test rig for heat transfer measurement is shown in Fig. 3. The test rig is mainly composed of a base frame with shafting mounted. The shafts were supported by two pairs of bearings. A coupling was used to connect the driving shaft at one side of the test sample to the AC motor, while the driven shaft and the brake disc are bolted to it. A cylindrical component modelling the knuckle with an outer diameter of 0.4 R_o was fabricated by using Perspex and was bolted to the mounting hub of the brake disc. A four channel slip ring was fixed to the driven shaft to connect the rotating heating pads attached to the rubbing surfaces with a power supply. Rotational speed of the brake disc was controlled by a frequency inverter and measured by a tachometer. More details of the test rig can be found in Ref. [23]. It should be noted that the present experimental configuration is somewhat different from a real braking test rig. However, relative merits between two brake discs independently uncovered by such a test rig and a braking test rig agree well with each other as detailed in Ref. [23]. Therefore, such a simplified experimental method is reasonable.

3.2. Heat transfer measurement method

To simulate frictional heating, two flexible heating pads consisting of Inconel heating wires and Kapton films were attached to both the inboard and outboard rubbing surfaces. Each Kapton film has a thickness of 0.076 mm and a thermal conductivity of 0.12 W/(mK) [24]. The constant heat flux (q'') of 3034 W/m^2 was imposed. To remedy the possible heat flux non-uniformity induced by the gaps between the heating wires, the aluminium foil having the thickness of 0.06 mm was attached to the outer surfaces of the heating pads. Afterwards, matt black paint was sprayed to the aluminium foils to ensure the emissivity of ~1.0. The temperature field on the inboard foil surface was measured by a calibrated

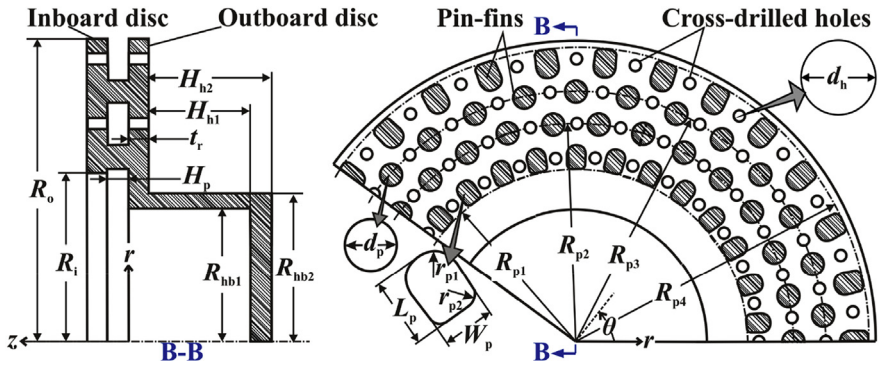

Fig. 2. Geometric details of the standard and cross-drilled brake discs with pin-fins.

Table 1
Detailed dimensions of the brake discs compared numerically in the present study.

Parameter	Value (mm)	Parameter	Value (mm)	Parameter	Value (mm)
d_h	5.0	r_{p1}	3.9/4.7	R_{p1}	93.0
d_p	9.8	r_{p2}	2.4/2.4	R_{p2}	113.4
H_{h1}	13.0	R_{hb1}	74.0	R_{p3}	127.4
H_{h2}	21.0	R_{hb2}	82.0	R_{p4}	147.0
H_p	10.0	R_i	90.0	t_r	9.0
L_p	10.6/12.6	R_o	150.0	W_p	8.3/9.8

Table 2
Detailed dimensions of the standard brake disc tested in the present study.

Parameter	Value (mm)	Parameter	Value (mm)	Parameter	Value (mm)
d_p	12.5	r_{p1}	5.0/6.0	R_{p1}	96.0
d_h	0.0	r_{p2}	3.0/3.0	R_{p2}	121.5
H_{h1}	56.5	R_{hb1}	73.0	R_{p3}	139.0
H_{h2}	68.5	R_{hb2}	82.0	R_{p4}	163.5
H_p	12.0	R_i	93.0	t_r	11.0
L_p	13.5/16.0	R_o	168.0	W_p	10.0/12.0

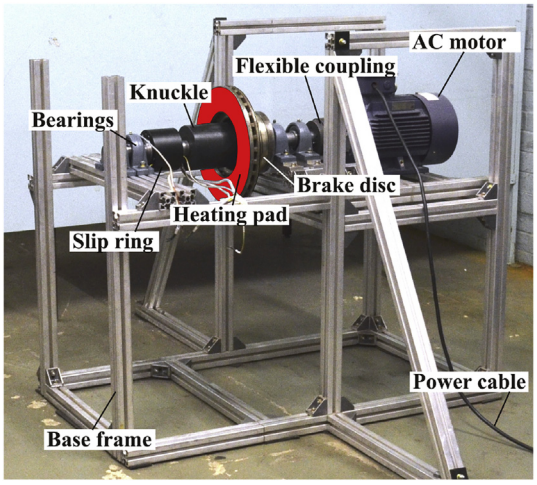

Fig. 3. The purposely built rotating test rig for thermal characterization of ventilated brake discs.

infrared camera, while reference ambient air temperature was measured by a T-type thermocouple. During the experiments, the rotational speed was varied from 200 to 1000 rpm, while reference air temperature was within 16–20 °C. More details on the heating pads, facilities, methods and operating conditions can be found in Refs. [21,23].

3.3. Data reduction and measurement uncertainties

The rotational Reynolds number (Re) and overall Nusselt number ($Nu_{overall}$) are adopted to characterize the overall cooling performance of the brake disc at various rotational speeds, separately defined as:

$$Re = \frac{\rho \omega R_o^2}{\mu} \tag{1}$$

$$Nu_{overall} = \frac{h_{overall} R_o}{k} \tag{2}$$

where ρ, μ and k are the density, dynamic viscosity and thermal conductivity of ambient air, respectively; ω is the angular velocity of the brake disc. The overall heat transfer coefficient ($h_{overall}$) is defined as:

$$h_{overall} = \frac{q''}{T_{rs,m} - T_a} - \frac{\varepsilon \sigma \left[T_{rs,m}^4 - T_a^4\right]}{T_{rs,m} - T_a} \tag{3}$$

where q'' denotes heat flux imposed by each heating pad; ε is the emissivity of the matt black paint; σ is Stefan-Boltzmann constant; $T_{rs,\,m}$ is the area-averaged rubbing surface temperature measured by the infrared camera; T_a is the ambient air temperature. During the numerical simulations, thermal radiation was not considered. Therefore, the contribution of thermal radiation to overall heat transfer was estimated and subtracted as indicated by the second term on the right hand side of Eq. (3).

For local heat transfer comparison between the experimental and numerical results, local effective heat transfer coefficient (h_e) and local effective Nusselt number (Nu_e) on the inboard rubbing surface are separately defined as:

$$h_e(r) = \frac{q''}{T_{rs}(r) - T_a} - \frac{\varepsilon \sigma \left[T_{rs}^4(r) - T_a^4\right]}{T_{rs}(r) - T_a} \tag{4}$$

$$Nu_e(r) = \frac{h_e(r) R_o}{k} \tag{5}$$

where T_{rs} is local rubbing surface temperature measured by the infrared camera. The contribution of thermal radiation to the local heat transfer is also subtracted as indicated by the second term on the right hand side of Eq. (4).

The root mean square method [25] has been used to estimate

measurement uncertainties. Following the specifications of the measurement instruments in Ref. [23], the maximum uncertainty for the angular velocity (ω), ambient air temperature (T_a) and average rubbing surface temperature ($T_{rs,m}$) were 5%, 0.5 °C and 0.3 °C, respectively. Consequently, the measurement uncertainty for the rotational Reynolds number (Re) were estimated to be within 5%, while those for the overall Nusselt number ($Nu_{overall}$) and local effective Nusselt number (Nu_e) were estimated to be less than 2.9%.

4. Details of the numerical simulation

For the cross-drilled brake disc, the presence of cross-drilled holes on the rubbing discs makes it difficult to fabricate a heating pad for heat transfer measurement. Therefore, this study carries out comparisons between the standard and cross-drilled brake discs by three-dimensional numerical simulations. Details of the numerical model are presented below.

4.1. Computational domain and boundary conditions

For both the brake discs rotating in ambient air, the geometries and the corresponding flow and temperature fields are rotationally periodic. Therefore, only a sector of each brake disc and the corresponding air around it was chosen as the computational domain with the central angle (θ_0) of 12°. As shown in Fig. 4, the axial and radial dimensions of the computational domain were decided to be $7(H_p+2t_r)$ and $2R_o$, which are large enough to eliminate the effects of the boundaries' locations on the flow and heat transfer near the brake disc according to the previous studies by Reddy et al. [10] and Wallis et al. [16]. To simulate heat generation inside the heating pads and the frictional heating, thin layers of heat source domains with identical thickness of 0.1 mm were attached to both the rubbing surfaces, where a constant volumetric heat source intensity based on the power input was specified. Other dimensions of these domains were identical to those of the rubbing surfaces. The thermal energy generated was transferred to both sides of these domains, which well represented the real situations.

Forasmuch as the Perspex knuckle has a low thermal conductivity, this part was not considered in the numerical model while adiabatic and no-slip boundary conditions were adopted for the knuckle walls. Due to the intrinsic nature of the flow and temperature in the computational domains, the rotational periodic condition was adopted for the periodic boundary pairs. For the upper, lower and outer boundaries of the computational domains as shown in Fig. 4, the opening conditions consisting of zero gauge pressure, atmospheric temperature and low turbulence intensity (1%) were specified in a rotating reference frame. Absolute flow direction was set to be perpendicular to the boundaries. Given that the absolute velocity magnitude far away from the brake disc is approximately zero, such opening conditions are reasonable. To include the thermal resistance induced by the Kapton films of the heating pads, thermal contact resistances were added at the interfaces among the heat source domains and the other domains. The values of the thermal resistances were determined by the thickness and thermal conductivity of the Kapton films provided in section 3.2. It should be noted that these contact resistances were only considered for the validation of the numerical model, which were removed during frictional heating simulations. For the other fluid-solid interfaces, the conservative interface flux condition was adopted.

4.2. Numerical methods

The multi-block structured mesh consisting of hexahedral elements was generated by ANSYS ICEM CFD to spatially discretize the computational domain. As shown in Fig. 5, fine mesh was generated near all the no-slip walls to sufficiently resolve the flow and thermal boundary layers. The height of the first layer of elements adjacent to the solid walls was approximately 0.1 mm. Relative coarse mesh was used far away from the walls. Smooth transition was ensured between the fine and coarse mesh regions. For the periodic surface pairs, one-to-one match of nodes was ensured.

The incompressible and steady-state conjugate heat transfer problem was solved by using ANSYS CFX 14.5 based on the finite volume method and the time marching algorithm. Governing equations were solved in a non-inertial reference frame rotating at the same rotational speed as that of the brake disc. The corresponding centrifugal and Coriolis forces were taken as source terms in the momentum equations. The high resolution scheme was selected to discretize the advection terms in the governing equations to reduce numerical error.

To reasonably predict the fairly complex flow field associated with the rotating brake discs, a model for the flow has to be carefully selected. Barigozzi et al. [15,26] measured the turbulence intensity distributions on several cylindrical cross-sections at the exit of a pin-finned brake disc by using hot-wire anemometer. The rotational speed of the brake disc was 750 rpm. Results indicated that the flow from the ventilated channel and the rubbing surface is prevalently turbulent. Previous studies [10,27] have shown that the

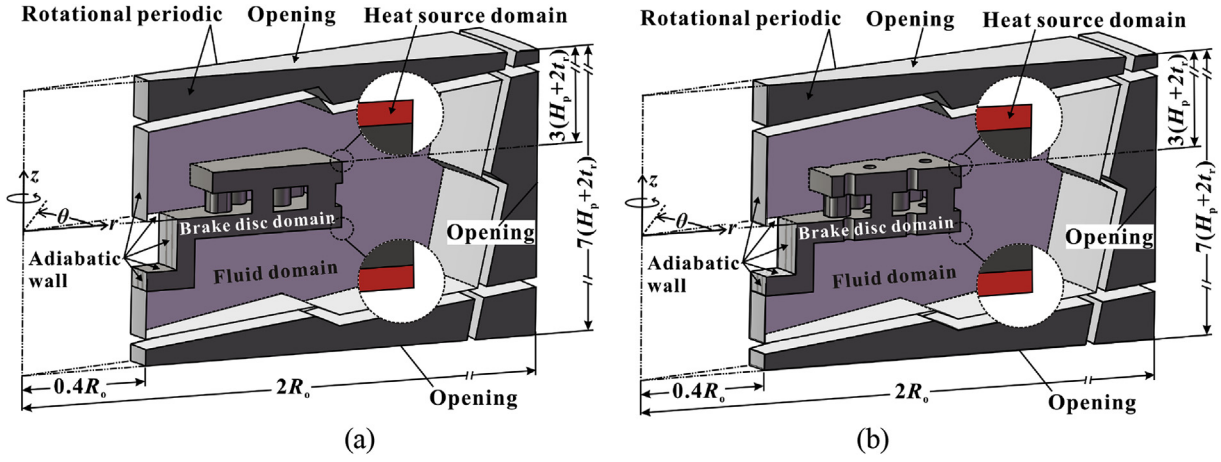

Fig. 4. The computational domain and boundary conditions adopted in the present simulations for: (a) the standard brake disc; (b) the cross-drilled brake disc.

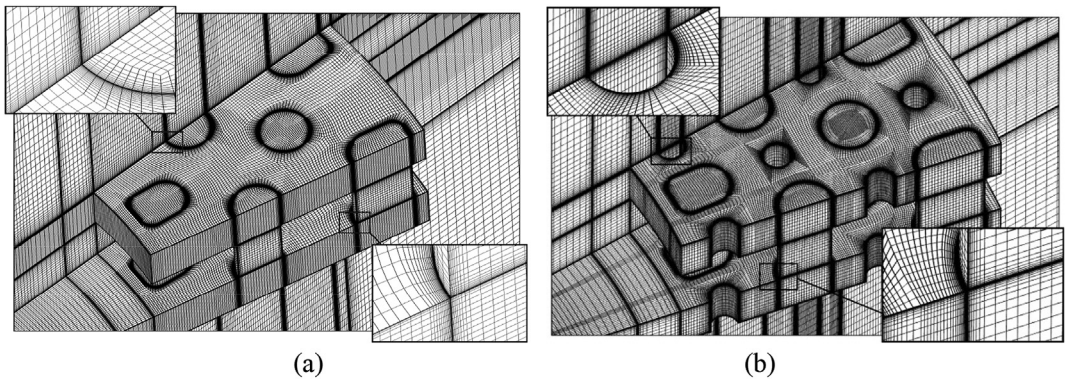

Fig. 5. The representative mesh used in the present simulation for: (a) the standard brake disc; (b) the cross-drilled brake disc.

Reynolds-averaged Navier-Stokes equations in conjunction with the turbulence models can well predict the flow field inside and outside the ventilated channels of the brake discs. The comparison between experimental and numerical data conducted by Mannohar Reddy et al. [27] indicated that the shear stress transport (SST model) [28] can well predict both the tangential and the radial velocity components at the exit of a ventilated brake disc. Similar comparisons made by these authors [10] also indicated that the SST model can well predict the flow inside of the ventilated channel. Furthermore, the present authors compared numerically and experimentally the cooling performances of a radial vane brake disc and a complex X-type lattice cored brake disc in Ref. [29], the relative merits uncovered by both data sets agreed very well with each other. In view of the above, the shear stress transport (SST) model was adopted for the flow with the dimensionless wall distance less than 1.0.

4.3. Mesh independency

For each brake disc, three sets of meshes were used to examine the effects of spatial resolution on the numerical results at the rotational speed of 1000 rpm. Regarding the standard brake disc, meshes with 3,197,168, 4,704,714 and 5,673,904 elements were considered. The overall Nusselt number showed a maximum deviation less than 1% among the three cases. For the cross-drilled brake disc, meshes with 5,313,306, 8,476,100 and 11823786 elements were considered. The overall Nusselt number from the last two meshes also exhibited a maximum discrepancy less than 1%. Therefore, meshes with 3,197,168 and 8,476,100 elements were finally adopted for the standard and cross-drilled brake discs, respectively.

5. Discussion of results

5.1. Enhanced overall cooling capacity by cross-drilled holes

To ensure a reliable comparison between the standard brake disc and the cross-drilled brake disc, validation of the numerical model is first performed. Fig. 6(a) presents the overall Nusselt number obtained experimentally and numerically for the commercial standard brake disc with its dimensions summarized in Table 2. The two datasets qualitatively and quantitatively show reasonable agreement, exhibiting a deviation of 0.3%–9.7%. Given that the measured distributions of the local effective Nusselt number (Nu_e) as defined in Eq. (5) showed a concentric pattern, Fig. 6(b) presents a comparison of the radial profile of Nu_e at two representative rotational speeds (N), i.e., 398 rpm and 769 rpm.

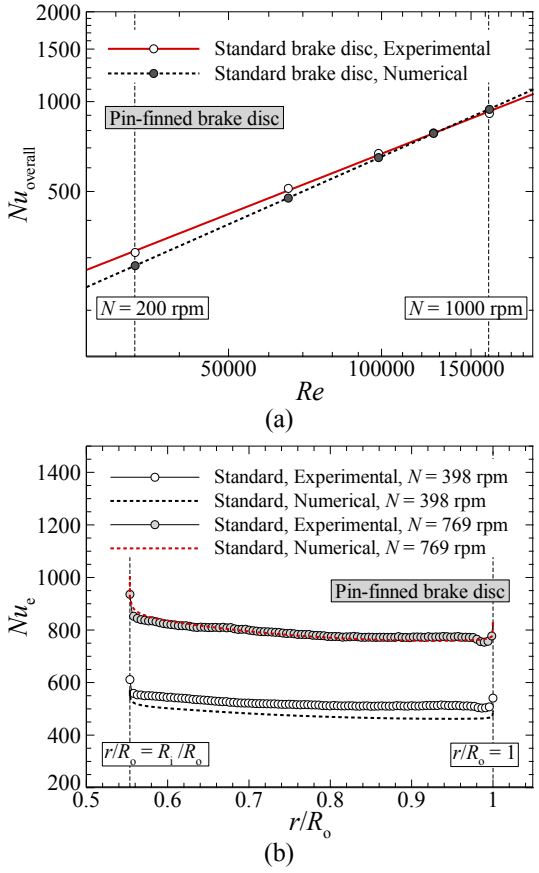

Fig. 6. Validation of the present numerical model via comparison between experimental and numerical results: (a) overall cooling performance; (b) radial profiles of local effective Nusselt number.

Qualitatively, the experimental data agree well with the experimental data. At the lower rotational speed, the deviation between the two data sets is within 9.7%. At the higher rotational speed, however, the discrepancy between the two data sets is negligible. Forasmuch as the same numerical strategy was adopted for both the brake discs, subsequent numerical comparisons are believed to be acceptable for the exploration of relative merits between the brake discs, especially at the rotational speed of 800 rpm.

Based on the validated numerical model, conjugate flow and heat transfer in both the standard and cross-drilled brake discs with the dimensions summarized in Table 1 were simulated. Fig. 7

depicts overall cooling performances of these brake discs. Within the typical operating range of 200–1000 rpm, the cross-drilled brake disc provides 15–17% higher overall Nusselt number relative to the standard brake disc. Therefore, the introduction of cross-drilled holes is beneficial to improve the cooling performance of the pin-finned brake disc.

5.2. Exploration of heat transfer enhancement mechanisms

For engineering optimization, clarification of the mechanisms underlying the improved cooling performance is of vital significance. Such insights can help the engineers to propose improved designs. Consequently, modification of the thermo-fluidic characteristics by the cross-drilled holes at the representative rotational speed of 800 rpm is explored in the non-inertial reference frame rotating at 800 rpm. Fluid flow behaviours are first discussed followed by local heat transfer characteristics.

Fig. 8 shows the surface streamlines and the non-dimensional pressure distributions on four cylindrical cross-sections for both the brake discs. In this figure, p denotes static pressure; and R_{h1} to R_{h4} denote radial locations of the axes of the cross-drilled holes, respectively. For the standard brake disc, it can be seen from Fig. 8(a) that the pressure inside the ventilated channel is generally lower than that near the rubbing surfaces of the discs as a result of the pumping effect of the pin-fins. Once the cross-drilled holes present, some fluid over the rubbing surface is driven into the ventilated channel through the cross-drilled holes due to the axial pressure gradient. The fluid through the cross-drilled holes first impinges onto the downstream edge of the hole inlet and then evidently flows along the pressure side of the hole surface. A recirculation region forms near the suction side of the hole surface due to flow separation. After the exit of the cross-drilled hole, the flow skewed towards the pressure side of the pin-fins. In contrast, for the cross-drilled radial vane brake disc, however, the through-hole flow skewed towards the suction side of each vane [21].

Fig. 9 presents the surface streamlines and the velocity distributions on an r-θ plane signifying the internal flow characteristics, where V denotes relative velocity magnitude. For both the brake discs, the flow skews towards the counter-rotating direction as a result of Coriolis force. The staggered pin-fin arrays act as in-line arrays in the brake discs. The mainstream flows around two sides of each pin-fin element, while a low-velocity flow recirculation region presents near leeside of each pin-fin as a result of flow separation. The flow ejected from the cross-drilled holes blocks and interacts with the mainstream entered from the inlet of the ventilated channel, which ultimately reduces the effective flow area and increases resistance of the mainstream flow. Therefore, velocity magnitude for the cross-drilled brake disc is generally lower than that of the standard brake disc due to reduced pumping capacity. In particular for the cross-drilled brake disc, the introduction of cross-drilled holes tends to transport fluid to the leading edges of the pin-fins as revealed by the high velocity region around the leading edges relative to the standard brake disc. The through-hole flow acts like a "cylinder" with mainstream flow around it, which is responsible for such a unique feature.

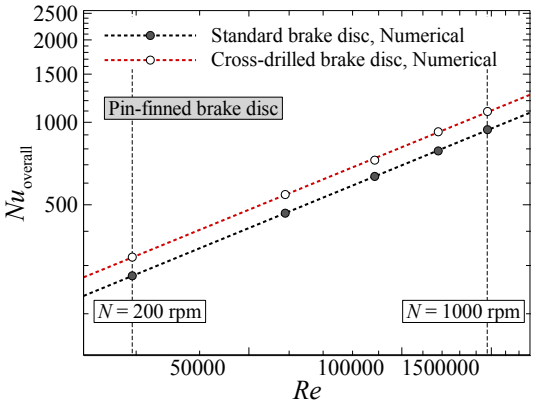

Fig. 7. Comparison of overall cooling performance between the standard and cross-drilled brake discs with pin-fin elements.

Fig. 10 shows a comparison of the velocity distribution on the r-θ plane 0.1 mm away from inner surface of the inboard disc, which is responsible for the local heat transfer on the inner disc surface. In general, the velocity magnitude for the cross-drilled brake disc is lower than that of the standard brake disc as a result of reduced pumping capacity. The smooth high velocity distribution along the flow path of the standard brake disc is interrupted by the cross-drilled holes; and a low velocity region is observable downstream each hole corresponding to the wake region of the through-hole flow. In addition, the high velocity region moves from two sides of each pin-fin for the standard brake disc to the leading edges for the cross-drilled brake disc.

Based on the aforementioned fluid flow characteristics, local heat transfer patterns on various surfaces of the brake discs are compared in detail, which imply the mechanisms underlying the enhanced overall cooling performance by cross-drilled holes. Fig. 11 first presents the local heat transfer patterns on the rubbing surfaces of both the brake discs. Hereafter, local Nusselt number is defined as that by Eq. (2) where the local heat transfer coefficient is based on the local heat flux, local wall temperature and ambient air temperature (T_a). It is evident that the introduction of cross-drilled holes enhances the local heat transfer within radial spans of the cross-drilled holes. When the boundary layer flow near the rubbing surface passes the cross-drilled holes, some low-momentum fluid is sucked into the ventilated channel. Thus thickness of the boundary layer circumferentially downstream each hole is reduced, which is responsible for the local heat transfer enhancement. Fig. 12 depicts local heat transfer distributions on the inner surface of the inboard disc, which correspond to the velocity distributions in Fig. 10. Downstream the first row of pin-fins, the high heat transfer region for the cross-drilled brake disc is smaller than that of the standard brake disc due to reduced pumping capacity. The high heat transfer regions near the pressure side of the pin-fins for the standard brake disc move towards the leading edges for the cross-drilled brake disc as a result of the aforementioned blockage effect. Fig. 13 presents the local heat transfer on the surfaces of the pin-fin elements, the first row of pin-fins exhibit a similar distribution for both the brake discs, because the flow around these pin-fins are not evidently affected by through-hole flow. However, the distributions on the surfaces of the rest pin-fins are evidently different. Corresponding to the fluid flow behaviors as shown in Fig. 9, the high heat transfer regions mainly present at the pressure sides of the pin-fins for the standard brake disc due to the shear by the high velocity smooth flow. For the cross-drilled brake disc, however, the high heat transfer regions are concentrated on the leading edges of the pin-fins, because the through-flow tends to transport fluid to the leading edges and increases local flow velocity.

Next, the modification of local heat transfer on different parts of the brake disc to the enhanced overall cooling performance can be quantified. The present numerical results reveal that the heat flow rate through the mid-height cross-section of the pin-fins is approximately zero; and therefore, only the inboard disc and half the pin-fins are considered. Hereafter, let numbers "1" to "6" denote the rubbing surface, the inner disc surface, the inner rim surface, the outer rim surface, the fin surface and the surface of the cross-drilled holes, respectively. From the energy balance of the

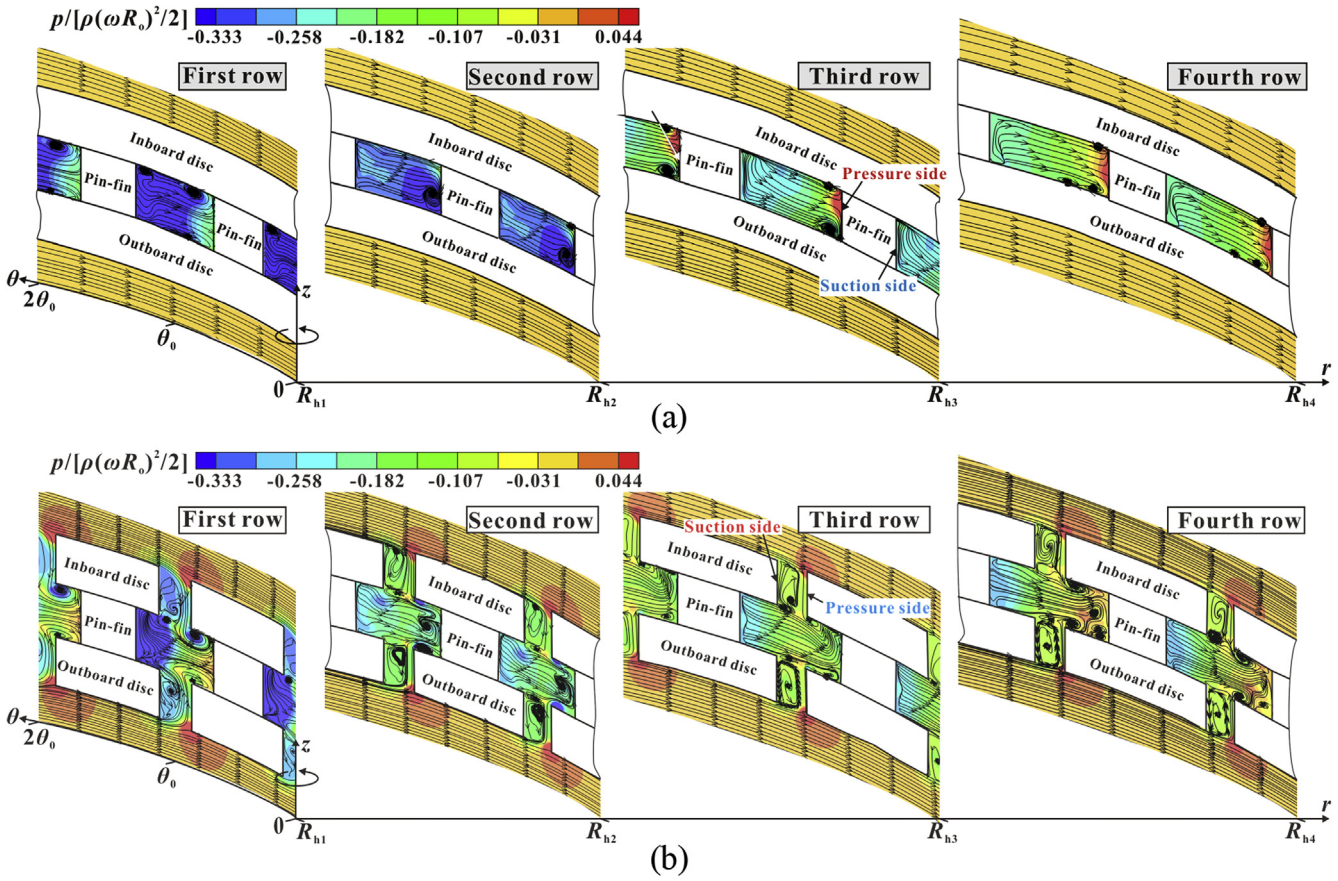

Fig. 8. Comparison of the fluid flow behaviors on four cylindrical cross-sections through axes of the cross-drilled holes: (a) the standard brake disc; (b) the cross-drilled brake disc.

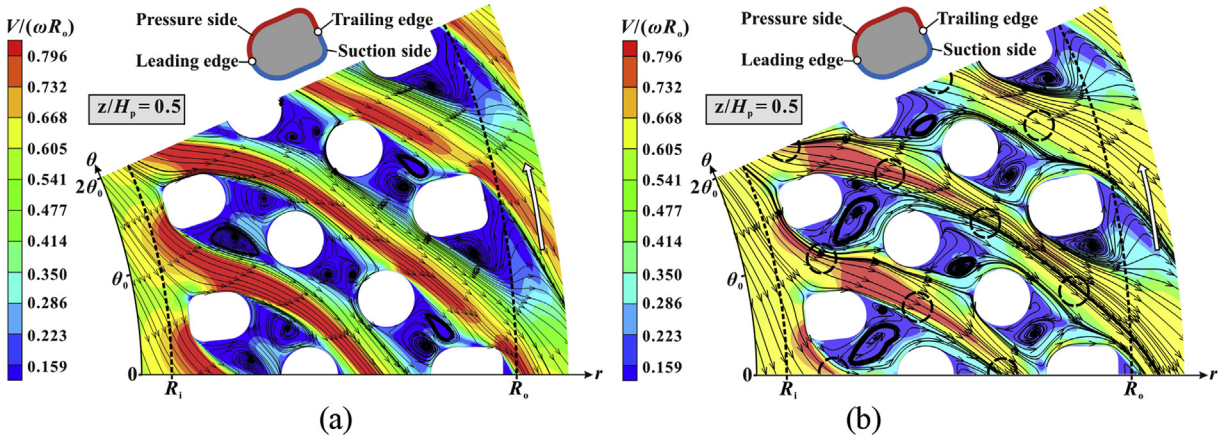

Fig. 9. Comparison of the fluid flow behaviors on the r-θ plane at $z/H_p = 0.5$: (a) the standard brake disc; (b) the cross-drilled brake disc.

selected system, the overall Nusselt number as defined in Eq. (2) can be decomposed as:

$$Nu_{\text{overall}} = \sum_{i=1}^{6} a_i b_i Nu_{i,\text{m}} \tag{6}$$

The coefficients a_i and b_i can separately be expressed as:

$$a_i = A_i/A_1 \tag{7a}$$

$$b_i = \left(\frac{T_{i,m} - T_a}{T_{1,m} - T_a}\right)\left\{\frac{\int_i [T_i(r,\theta,z) - T_a]h_i(r,\theta,z)dA}{\int_i [T_i(r,\theta,z) - T_a]dA}\frac{1}{h_{i,m}}\right\} \tag{7b}$$

In the above equations, $Nu_{i,\text{m}}$, A_i, $T_{i,\text{m}}$, T_i, $h_{i,\text{m}}$ are average Nusselt number, heat transfer area, average temperature, local temperature and average heat transfer coefficient on a specific surface,

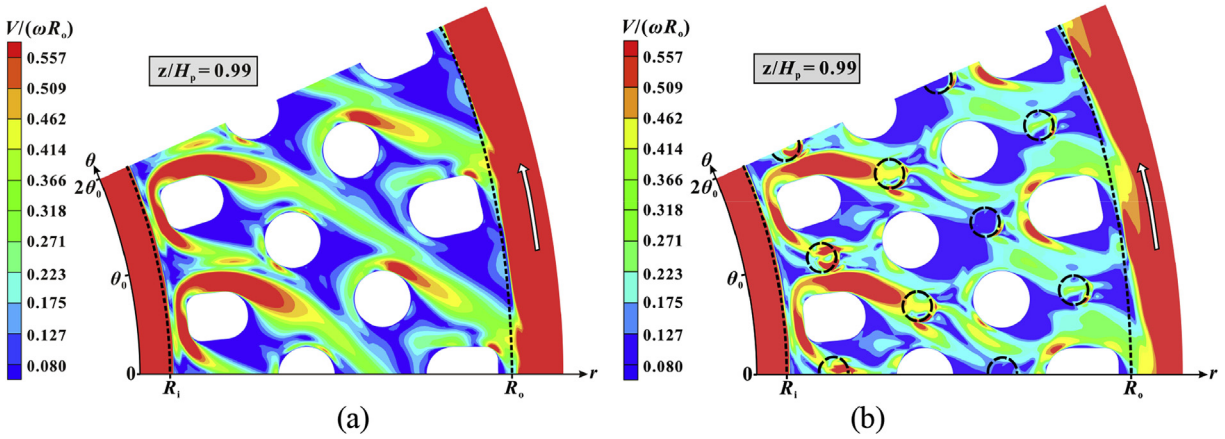

Fig. 10. Comparison of fluid flow behaviors on the r-θ plane at $z/H_p = 0.99$: (a) the standard brake disc; (b) the cross-drilled brake disc.

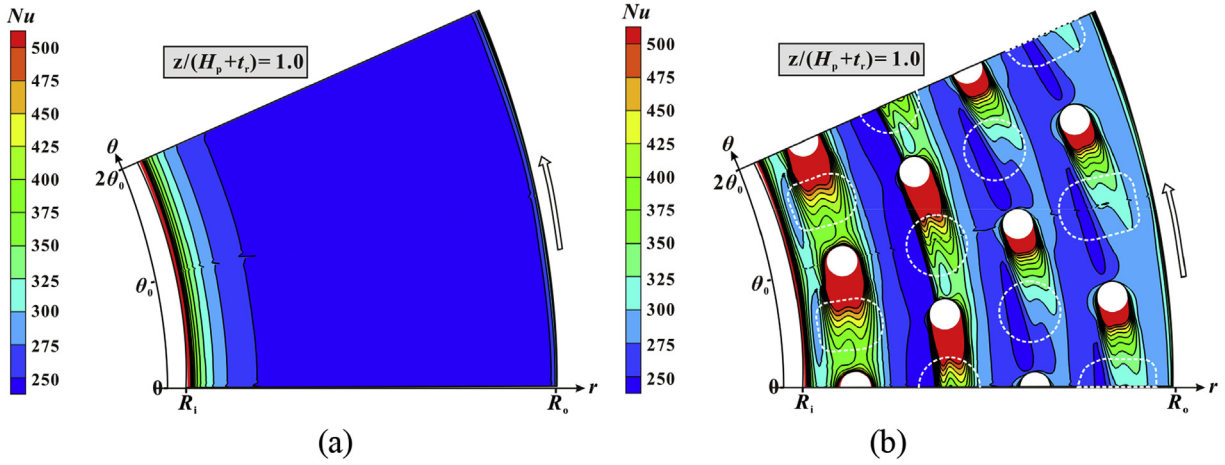

Fig. 11. Comparison of the local heat transfer distribution on the rubbing surface of the inboard disc: (a) the standard brake disc; (b) the cross-drilled brake disc.

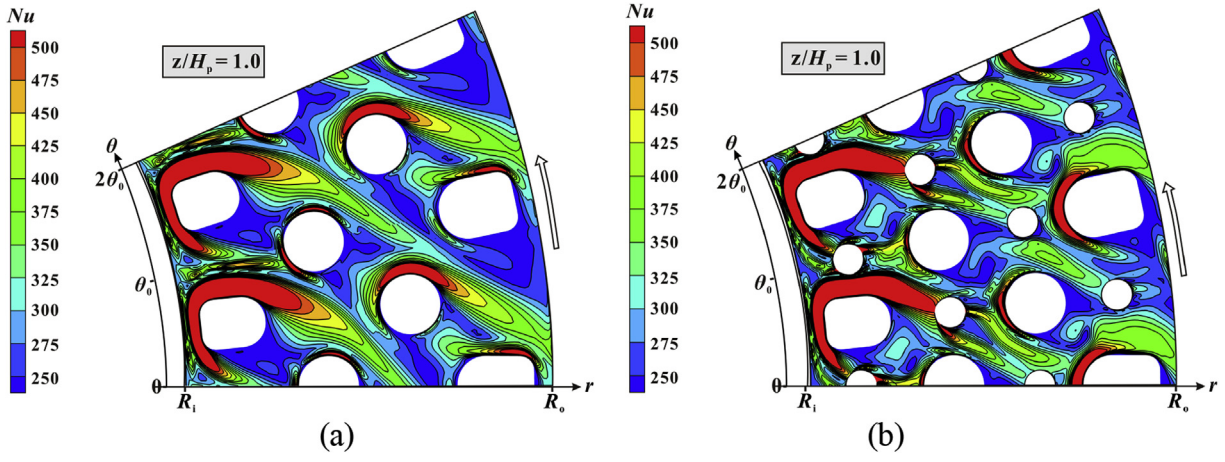

Fig. 12. Comparison of the local heat transfer distribution on the inner surface of the inboard disc: (a) the standard brake disc; (b) the cross-drilled brake disc.

respectively. For the standard brake disc, the values of $Nu_{i,\,m}$, a_i and b_i are assumed to be zero. Then the contribution of the local heat transfer variation on a specific surface to the overall heat transfer enhancement (η_i) can be quantified as:

$$\eta_i = \frac{(a_i b_i Nu_{i,m})_{cross-drilled} - (a_i b_i Nu_{i,m})_{s\ \tan\ dard}}{\left(\sum_{j=1}^{6} a_j b_j Nu_{j,m}\right)_{s\ \tan\ dard}} \tag{8}$$

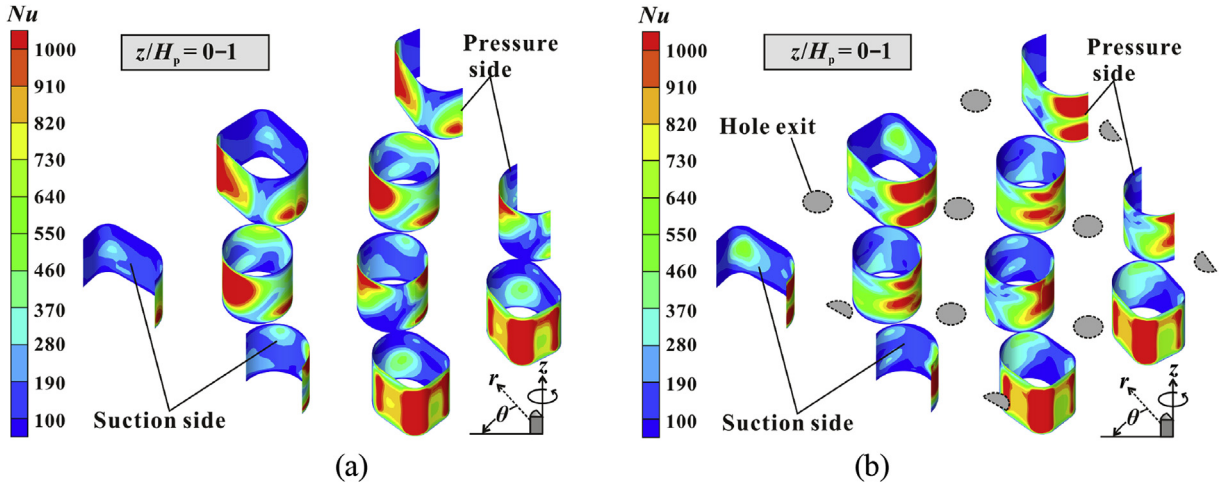

Fig. 13. Comparison of the local heat transfer distribution on the surface of the pin-fins: (a) the standard brake disc; (b) the cross-drilled brake disc.

As quantified in Fig. 14 based on Eq. (8), local heat transfer on inner disc surface, pin-fin surface, inner rim surface and outer rim surface are deteriorated mainly due to the reduced pumping capacity. Their negative contributions to the enhanced cooling performance of the cross-drilled brake disc are −2.39%, −1.11%, −0.63% and −0.21, respectively. However, improved heat transfer on the rubbing surface and the additional heat transfer on the surface of the cross-drilled holes positively contribute 8.35% and 12.65% to the overall heat transfer enhancement.

5.3. Systematic comparison with radial vane brake discs

The radial vane and the pin-finned ventilated brake discs are prevalent bidirectional ventilated brake discs in modern vehicles. However, to the best knowledge of the present authors, a comprehensive comparison among the standard and cross-drilled brake discs with these two kinds of heat dissipation elements are not yet available in the open literature. The main issue is that existing vague studies generally do not provide geometric details of the brake discs and even experimental/numerical details as reviewed previously in the introduction. Therefore, this section presents a clear and systematic comparison among four brake discs as a complement. It should be mentioned that the radial vane brake disc in Ref. [21] with detailed geometric parameters has identical core porosity to that of the pin-finned brake disc in the present study. As shown in Fig. 15, for the radial vane brake disc, the introduction of cross-drilled holes enhances the overall cooling capacity by 22–27% [21], while for the pin-fined brake disc, the superiority of the cross-drilled brake disc relative to the standard one is 15–17%. The cross-drilled pin-finned brake disc exhibits similar overall cooling performance to the standard radial vane brake disc. The cross-drilled radial vane brake disc provides the best cooling performance.

For the radial vane brake disc, a large flow recirculation region with low static pressure forms near suction side of each vane where cross-drilled holes are configured [21]. However, for the present pin-finned brake disc, high velocity smooth flow dominates near both the pressure and suction sides of each pin-fin (see Fig. 9). For a given rotational speed, therefore, local static pressure at the exit of the cross-drilled holes for the radial vane brake disc is lower than that for the pin-finned brake disc. Thus the greater axial pressure gradient for the radial vane brake disc allows more coolant to enter the cross-drilled holes. In view of such a fact and the aforementioned mechanisms in section 5.3, the introduction of cross-drilled holes has a more evident yet positive effect on local heat transfer on the rubbing surface and hole surface of the radial vane brake disc. In addition, for both the radial vane and the pin-finned brake discs, the through-hole flow blocks the mainstream from the ventilated channel inlet and therefore, deteriorates the local heat transfer on

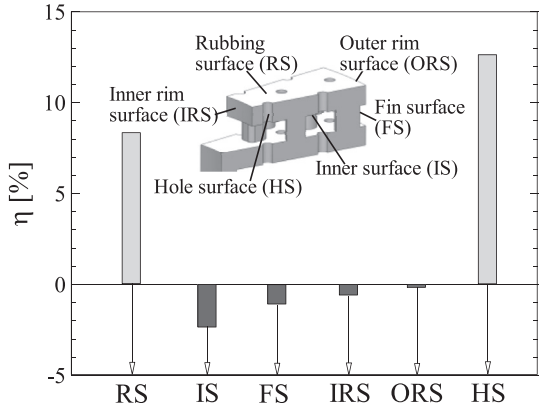

Fig. 14. Quantitative contributions (η) of the modified heat transfer on various surfaces to enhanced overall cooling performance of the cross-drilled pin-finned brake disc.

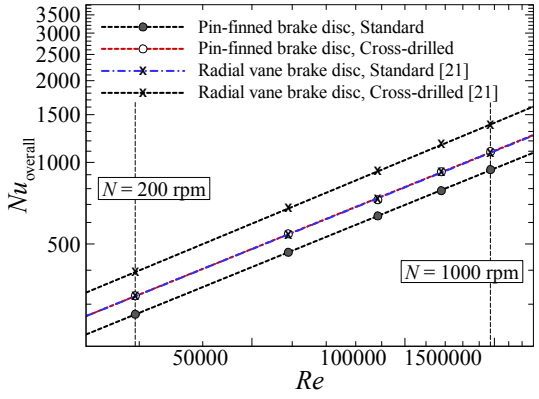

Fig. 15. Systematic comparison of overall cooling performance between the present pin-finned brake discs and the radial vane brake discs in Ref. [21] having identical core porosity.

the inner surface of the rubbing disc. However, the deterioration of local heat transfer for the radial vane brake disc is more evident due to higher mass flow rate through its cross-drilled holes. Under the effects of the above factors, the introduction of cross-drilled holes enhances overall cooling performance of the radial vane brake disc to a greater extent relative to the pin-finned brake disc. Initially, the standard pin-finned brake disc exhibits inferior overall cooling performance to that of the standard radial vane brake disc. Once cross-drilled holes are introduced, the cross-drilled pin-finned brake disc finally has a similar cooling performance to that of the standard radial vane brake disc.

Motivated by the above facts, improved designs of the cross-drilled pin-finned brake disc may be proposed. Now that a large flow recirculation region with low pressure forms hydraulically downstream each pin-fin as revealed by Fig. 9(a), placing the cross-drilled holes in this region is expected to enhance mass flow rate through the holes. Consequently, the heat transfer on the rubbing surface and the surface of the holes can be improved. The through-hole flow can feed coolant to the flow recirculation region which is beneficial to improve the local heat transfer on the surfaces around this dead-flow region. However, such a configuration will make the brake disc unidirectional. Fortunately, as revealed by Fig. 14, placing cross-drilled holes along the high velocity mainstream path is always beneficial for cooling performance. Therefore, additional holes symmetrical with the aforementioned holes relative to the *r-z* symmetry plane of each pin-fin can be introduced. Thus the brake disc will be bidirectional again. Further, to mitigate the heat transfer deterioration on the inner surface of the rubbing disc due to blockage of mainstream flow by the through-hole flow, the inclination of the hole axis to the direction of the mainstream flow may be better. Finally, putting the holes closer to the ventilated channel is expected to be more effective. Improved designs according to the above suggestions are expected to further improve the cooling performance of the pin-finned brake disc. Further investigations will be presented in subsequent studies.

6. Conclusions

To further understand the effect of cross-drilled holes on the cooling performance of ventilated brake discs, this study has presented a detailed thermo-fluidic comparison between standard and cross-drilled pin-finned brake discs. Subsequently, a systematic comparison between the radial vane and the pin-finned brake discs with/without cross-drilled holes has been conducted. Conclusions drawn from this study are summarized as follows.

(1) The cross-drilled pin-finned brake disc provides 15–17% higher steady-state cooling capacity relative to the standard pin-finned brake disc.
(2) The suction of ambient air into the ventilated channel lowers the static pressure inside the ventilated channel, which leads to an axial pressure gradient. With the presence of cross-drilled holes, the low-momentum fluid near the rubbing surfaces is driven into the ventilated channel. Correspondingly, thickness of the thermal boundary layer over the rubbing surfaces decreases; and therefore, local heat transfer within radial spans of the cross-drilled holes is evidently enhanced for the rubbing surfaces. In addition, the through-hole flow removes a large portion of heat from the additional surface of the cross-drilled holes.
(3) The through-hole flow injected into the ventilated channel blocks the mainstream from the ventilated channel inlet and therefore introduces additional resistance to the mainstream. As a result, pumping capacity from the inlet of the ventilated channel decreases. Consequently, local heat transfer on other surfaces is slightly deteriorated.
(4) The cross-drilled pin-finned brake disc exhibits similar cooling performance to the standard radial vane brake disc, while the cross-drilled radial vane brake disc provides the best overall cooling capacity. The introduction of cross-drilled holes poses more evident and positive effect on the radial vane brake disc.

Acknowledgements

This research was supported by the Fundamental Research Funds for the Central Universities (3102016QD058) and the National 111 Project of China (Grant No: B06024). The authors would like to thank Prof. Tongbeum Kim from University of the Witwatersrand for his kindly help on this work.

References

[1] Lee K. Numerical prediction of brake fluid temperature rise during braking and heat soaking, SAE Technical Paper No. 1999-01-0483.
[2] Ahmed I, Leung PS, Datta PK. Experimental investigations of disc brake friction, SAE Technical Paper No. 2000-01-2778.
[3] Cho MH, Kim SJ, Basch RH, Fash JW, Jang H. Tribological study of gray cast iron with automotive brake linings: the effect of rotor microstructure. Tribol Int 2003;36(7):537–45.
[4] Anoop S, Natarajan S, Kumaresh Babu SP. Analysis of factors influencing dry sliding wear behaviour of Al/SiC_p-brake pad tribosystem. Mater Des 2009;30(9):3831–8.
[5] Okamura T, Yumoto H. Fundamental study on thermal behavior of brake discs, SAE Technical Paper No. 2006-01-3203.
[6] Mackin TJ, Noe SC, Ball KJ, Bedell BC, Bim-Merle DP, Bingaman MC, et al. Thermal cracking in disc brakes. Eng Fail Anal 2002;9(1):63–76.
[7] Gao CH, Huang JM, Lin XZ, Tang XS. Stress analysis of thermal fatigue fracture of brake disks based on thermomechanical coupling. ASME J Tribol 2007;129(3):536–43.
[8] Kao TK, Richmond JW, Douarre A. Brake disc hot spotting and thermal judder: an experimental and finite element study. Int J Veh Des 2000;23(3–4):276–96.
[9] Belhocine A, Bouchetara M. Thermal behavior of full and ventilated disc brakes of vehicles. J Mech Sci Technol 2012;26(11):3643–52.
[10] Reddy SM, Mallikarjuna JM, Ganesan V. Flow and heat transfer analysis of a ventilated disc brake rotor using CFD, SAE Technical Paper No. 2008-01-0822.
[11] Palmer E, Mishra R, Fieldhouse J. A computational fluid dynamic analysis on the effect of front row pin geometry on the aerothermodynamic properties of a pin-vented brake disc. IMechE J Automob Eng 2008;222(7):1231–45.
[12] Chatterley TC, Macnaughtan MP. Cast iron brake discs—current position, performance and future trends in Europe, SAE Technical Paper No. 1999-01-0141.
[13] Thomas TH. Disc brakes “two years after”, SAE Technical Paper No. 670197.
[14] Barigozzi G, Cossali GE, Perdichizzi A, Boden A, Pacchiana P, Experimental investigation of the mean and turbulent flow characteristics at the exit of automotive vented brake discs, SAE Technical Paper No. 2002-01-2590.
[15] Barigozzi G, Cossali GE, Perdichizzi A, Lorenzo S, Pacchiana P. Experimental investigation of the aero-thermal characteristics at the exit of an automotive vented brake disc, SAE Technical Paper No. 2003-01-3338.
[16] Wallis L, Leonardi E, Milton B, Joseph P. Air flow and heat transfer in ventilated disc brake rotors with diamond and tear-drop pillars. Numer Heat Transf A Appl 2002;41(6–7):643–55.
[17] Palmer E, Mishra R, Fieldhouse J. An optimization study of a multiple-row pin-vented brake disc to promote brake cooling using computational fluid dynamics. IMechE J Automob Eng 2009;223(D7):865–75.
[18] Wallis L. A comparison of bi-directional disc brake rotor passage designs. Ph.D. thesis. Sydney, Australia: The University of New South Wales; 2003. p. 90–8.
[19] Antanaitis D, Rifici A. The effect of rotor crossdrilling on brake performance, SAE Technical Paper No. 2006-01-0691.
[20] Barigozzi G, Perdichizzi A, Pacchiana P, Goller R. Aero-thermal characteristics of an automotive CCM vented brake disc, SAE Technical Paper No. 2005-01-3930.
[21] Yan HB, Feng SS, Yang XH, Lu TJ. Role of cross-drilled holes in enhanced cooling of ventilated brake discs. Appl Therm Eng 2015;91:318–33.
[22] Kim SW, Park K, Lee SH, Kang KH, Lim KT. Thermophysical properties of automobile metallic brake disc materials. Int J Thermophys 2008;29:2179–88.
[23] Yan HB, Mew T, Lee M-G, Kang K-J, Lu TJ, Kienhöfer FW, et al. Thermofluidic characteristics of a porous ventilated brake disk. ASME J Heat Transf 2015;137(2). 022601-1–;022601–11.
[24] Lyall ME. Heat transfer from low aspect ratio pin-fins. Master thesis. Blacksburg, USA: Virginia Polytechnic Institute and State University; 2006.
[25] Coleman HW, Steele WG. Experimentation, validation, and uncertainty

analysis for engineers. third ed. Hoboken, New Jersey: John Wiley & Sons Inc.; 2009.
[26] Barigozzi G, Perdichizzi A, Donati M. Combined experimental and CFD investigation of brake discs aero-thermal performances. SAE Int J Passeng Cars 2008;1(1):1194–201.
[27] Reddy SM, Mallikarjuna JM, Ganesan V. Flow and heat transfer analysis through a brake disc—a CFD approach. In: Proceedings of the ASME 2006 international mechanical engineering congress and exposition, vol. 3. Chicago, Illinois, USA: ASME; 2006. p. 481–5.
[28] Menter FR. Two-equation eddy-viscosity turbulence models for engineering applications. AIAA J 1994;32(8):1598–605.
[29] Yan HB, Zhang QC, Lu TJ. Heat transfer enhancement by X-type lattice in ventilated brake disc. Int J Therm Sci 2016;107:39–55.